An approach for uniting bottom-up and top-down systems and its applications

Akira Ishibashi

Research Institute for Electronic Science, Hokkaido University, Sapporo, Hokkaido 001-0020
Dept. of Physics, Faculty of Science, Hokkaido University, Hokkaido 060-0810
C'sTEC Corporation, 2-20, N8W6, Sapporo, Hokkaido 060-0808, Japan
Email: i-akira@es.hokudai.ac.jp

Abstract— *We have investigated the possibility of creating a unification platform for top-down systems and bottom-up structures, which is one of the most important issues for harvesting fruits of upcoming nano-technologies and nano-science together with those of Si- LSI-based information technologies. Under the device-approach, for unifying bottom-up and top-down systems, proposed is a functional device that has hierarchical structures grown, or is to have hierarchical structures grow, inside, not as a result of top-down designing but as a result of self-organization, i.e., a bottom-up structure-formation. Spiral heterostructure is of potential interest for providing us with one-dimensional superlattice structure that would serve as a bridge between top-down LSI systems with two-dimensional bottom-up structures. The spiral heterostructure is, also, of importance for enabling multi-striped orthogonal photon-photocarrier-propagation solar cell (MOP^{3}SC). On the other hand, as a tool-based approach, for unifying bottom-up and top-down systems, clean unit system platform (CUSP) is developed. CUSP can realize dust- and microbe-free environment. The clean versatile environments having small footprint, low power-consumption and high cost-performance can be realized with CUSP for the next generation production system as well as for cross-disciplinary experiments. The approach for uniting bottom-up and top-down systems gives not only new devices but also clean platforms that would be able to serve as clean space for all of us.*

Keywords— Top-down system, Bottom-up structure, device-based approach, spiral heterostructure, tool-based approach, clean unit system platform, CUSP.

I. INTRODUCTION

A possible platform that unites, or makes a bridge over the gap between, the top-down systems such as Si-based LSIs, for which lithography plays vital roles, and bottom-up systems like self-organized or self-assembled systems will surely be able to enjoy as huge a success as the string theory does, because of its full seamless line-up of highly structured materials. First, we have to overcome the sharp contrast lying between the top-down system, the structure of which is fabricated globally through man-made design from outside by so-called processing, and the bottom-up system, for which the structure, on the other hand, is determined autonomously through the local interactions described by non-equilibrium diffusion equations, etc. Study of the possibility of creating a unification platform for bottom-up and top-down systems is one of the most important issues, in future, for harvesting the fruits of upcoming nano-technologies and nano-science together with those of Si-LSI-based information technologies.

Conventional mainstream functional devices are those manufactured by a top-down approach based upon micro-fabrication, as represented by semiconductor integrated circuits. Especially regarding semiconductor devices, huge semiconductor electronics industry has been established, via inventions of transistors [1], and inventions of semiconductor integrated circuits [2,3]. On the other hand, the top-down approach begins to see delimitation in various points. As a technique that breaks the limit, a bottom-up approach by self-organization, etc. has been remarked and studied actively. Both cell systems and neuron systems have been reported to continuously expand and grow by autonomous dispersion at individual sites [4]. This is classified as bottom-up systems. In bottom-up systems, individual portions independently build structures according to local rules or interactions that lead to autonomous decentralized systems. It has been demonstrated by using cellular automaton that there are four different types of structure-building schemes (constant, periodically laminated [nested], functionally structured, and random) with respect to time [5]. Also with respect to time, especially based upon the concept of time projection, we have reported an improvement of a time projection chamber (TPC) as an elementary particle detector using secondary electrons continuously moving with time (electrons generated along trajectories of elementary particles), based on constancy of the drift velocity [6]. On the other hand, it has also been reported that resolution of a one-atomic layer in the growth direction is obtained in growth of a semiconductor using metal organic chemical vapour deposition (MOCVD) [7]. Also reported was a structure inserting a molecular element at a crossing point of approximately 40 nm wide metal wires put

crosswise [8]. Further, as another example of bottom-up schemes, there have been proposed a method of building structures by self-organized progressive hierarchical acquisition (SOPHIA) [9] and a method of growing neurons. In addition, there is gene-governed expression of configurations (gene-derived structures) universal to life and biological systems. On the other hand, as other examples of the top-down systems, there are MEMS systems (micro electromechanical systems), micro-chemical reactors, and building of structures by human brains (brain-derived structures) as *homo faber*, in general [10].

II. TOP-DOWN STRUCTURES AND BOTTOM-UP STRUCTURES

2.1 Top-down structures

As widely known, two-dimensional patterning by photolithography is ofien used in the manufacture of semi-conductor devices by the top-down approach. Figure 1 shows schematically LSI (memory, for example) as an example of a semiconductor device. As shown in Fig. 1, two dimensional patterning is usually conducted by using ultra-violet (UV) or extreme ultraviolet (EUV) photolithography, or electron beam lithography, at one time at each point of time, i.e., instantaneously at each time of each elementary process such as batch exposure, development, etching, and so on, at individual points on a time axis, under no exchange of information in spatially lateral direction in the surface of the semiconductor substrates. That is, one of large characteristics of two-dimensional patterning is to weave the time into structures discontinuously and sporadically, i.e., the time is projected discontinuously. We can analyze the situation in the three-dimensional (3D) coordinates, i.e., time axis, space (or structure) axis, and the development-rate-axis (or variation axis) as shown in Fig. 1.

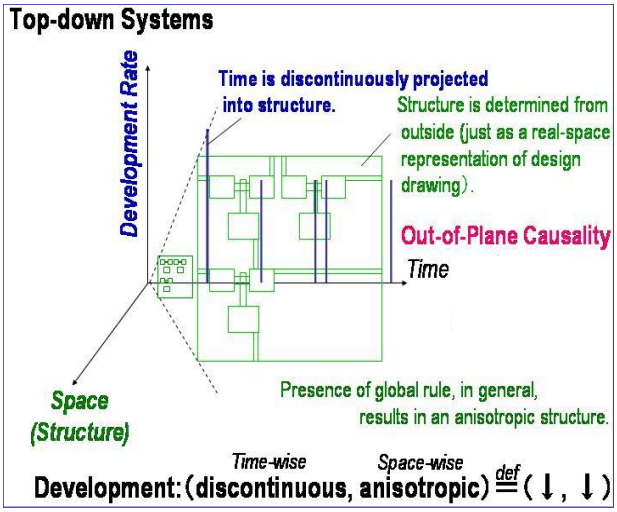

FIGURE 1: SCHEMATIC DRAWING OF AN LSI CONSIDERED IN THE THREE DIMENSIONAL (3D) COORDINATES, I.E., TIME AXIS, SPACE AXIS, AND THE DEVELOPMENT-RATE-AXIS

In two-dimensional patterning, for example, configuration of a structure is determined by photo-lithography through batch exposure of a photo-resist using a photo mask. Therefore, upon building a structure, there is no exchange of information in lateral directions among the in-plane structures. More specifically, causality mainly exists, thanks to the photo-mask, in interaction in the vertical direction relative to the substrate plane (we can call this out-of-plane causality) and not in the in-plane direction. In the two-dimensional patterning, block structures are produced under a global rule provided by photo-lithography as shown in Fig. 1, and there is a particular directionality for each block. Therefore, the spatial configuration is anisotropic, in general, from both microscopic and macroscopic viewpoints. In other words, configuration of the structure is determined by extrinsic factors, and it is a just real-spatial expression of a circuit design generated, originally, in human-brain. In addition, structural changes on the substrate become a series of pulses in form of a δ-function with respect to the time. Thus, the top-down systems are characterized as an anisotropic (directional) structures which time is projected (or woven into) discontinuously to, and is anisotropic in space-wise. Let a system be expressed by ↑ when having time continuous projectivity or spatial isotropy, and let a system be expressed by ↓ when having time discontinuous projectivity or spatial anisotropy. Then the top-down system can be characterized by (time projectivity, spatial directionality) = (↓, ↓), i,e., the system is discontinuous in time-wise and anisotropic in space-wise. In other words, since in a top-down system the time is discontinuously projected and there exists the spatial anisotropy in general, it is well-approximated as (time projectivity, spatial directionality) = (↓, ↓). Laser diode is another example of the top-down system, because they are fabricated through optical lithography and semiconductor processing just like the aforementioned Si-based LSIs.

2.2 Bottom-up structures

On the other hand, another stream whose importance has been remarked recently is so-called bottom-up systems. The systems include self-organized systems, for example, composed of inorganic substances, such as those represented by semiconductor quantum dots. As an example of bottom-up systems, urine bladder epithelium is shown in Fig. 2. Such bottom-up systems are well-known to continuously enlarge and grow with time by autonomous dispersion [4].

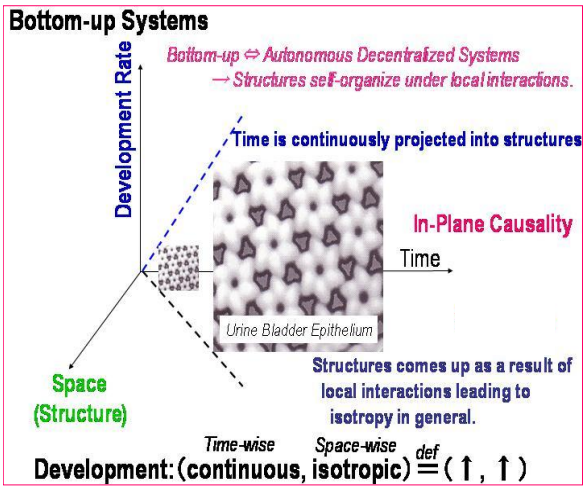

FIGURE 2: SCHEMATIC DRAWING OF AN LSI CONSIDERED IN THE 3D-COORDINATES, I.E., TIME AXIS, SPACE AXIS, AND THE DEVELOPMENT-RATE-AXIS

As shown in Fig. 2, in bottom-up structures characterized by the nature of autonomous decentralized systems, the individual subsystems/portions automatically form structures according to the local rules/interactions. Therefore, time is projected (or woven) into the structure continuously. In this case, in a bottom-up structure like vesical epidemic cells having a two-dimensional extension similar to that of Fig. 2, causality exists in the plane (we call this in-plane causality). As Wolfram has shown by using a cellular automaton, there are four different types I to IV (constant, periodically laminated [nested], functionally structured and random) as formation of structures [5]. In the bottom-up systems, since formation of structures follows local rules/interactions and has no particular directions from the global viewpoint, the spatial configurations usually become, in general, isotropic. In this case, the entire structure is determined by intrinsic factors according to the generation rule. Changes of structures exhibit a smooth continuous line with respect to time, i.e., time is projected continuously into structure. Thus, as shown in Fig. 2, bottom-up systems are in general at least within an intermediate range isotropic (undirectional) structures to which time is projected continuously. Therefore, according to the above notation, they can be expressed as (time projectivity, spatial directionality) = (↑,↑) in the 3D-space aforementioned as shown in Fig. 2. In general, living matters of life forms adequately combine the bottom-up properties based upon the body systemizing characteristics governed by genes. More specifically, the living matters integrate the bottom-up capability in formation of body tissues in the growth of individuals from fertilized eggs through the long course of evolution, which is a typical biological system but there is non-biological case, too.

Thus, another example of bottom up systems is structures emerging in degrading II-VI laser diodes. When current is injected in LD's for a long period of time in aging experiment, the LD's degrade with respect to their device performance, i.e., more amount of current needs to be injected to maintain a constant output power. Those degradations are due to recombination enhanced defect reactions, as first seen long time ago in AlGaAs-based laser diodes [11], and also in materials such as InGaAsP and in ll-VI [12,13]. The degradation, or we would rather say, aging of the LD's can be regarded as one of the self-organized criticality and that the resultant dislocation network, being one of bottom-up structures, can be built into the top-down structure of the LD's in a well-controlled manner as shown below.

A transmission electron micrograph (TEM) image of an active region of degraded ZnMgSSe-based LDs is shown in Fig. 3. The fabrication process is given elsewhere [14]. In the degraded active layer of the LD's are seen dislocation networks consisting of many self-similar, nested V-shaped structures with different sizes, i.e., the dislocation network has a fractal structure. Those dislocations are responsible for the increase in operating current in aging experiment at a constant output-

power. The starting point of the dislocation network is pre-existing defects, i.e., stacking faults starting at the epi/sub. interface [12,13]. Numbers of the V-shaped structures are plotted with respect to the size in Fig. 4. The inset shows the result obtained through box counting method. As shown in Fig. 4, a power-law, just like the one demonstrated with sand pile model [14], holds for the numbers and the sizes of the V-shaped dislocation structure. The dislocation network starts from the stacking fault and is found, from Fig. 4, to have a fractal dimension ~ 1.55 indicating the aging process, or the degradation of LD, is one example of the self-organized criticality seen universally in systems having energy in-flow and spatio-temporal dissipation, i.e., the current injection and non-radiative recombination at defect sites, respectively, in the present case. With current injection into the pn-junction region of LD device, nested V-shaped dislocation network grows and as the time of current injection gets longer, the range in which the power law holds becomes wider. The LDs' aging, on one hand, is deterioration in device performance, but, on the other hand, it reflects the increasing complexity at pre-existing defect sites.

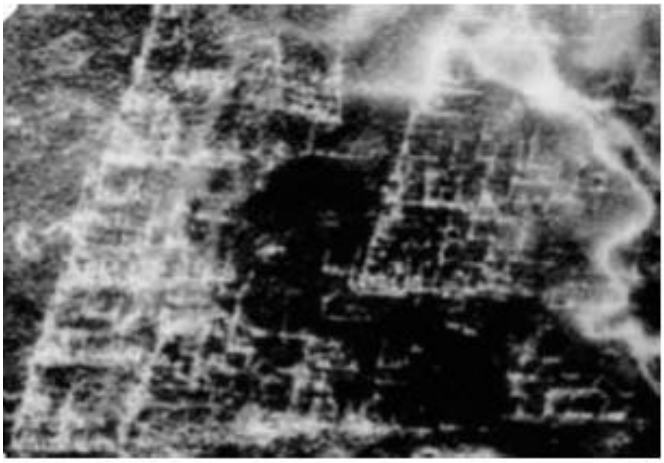

FIGURE 3: TEM IMAGE OF DEGRADED II–VI LASER DIODE. MANY SELF-SIMILAR V-SHAPED STRUCTURES ARE SEEN WITH DIFFERENT SIZES

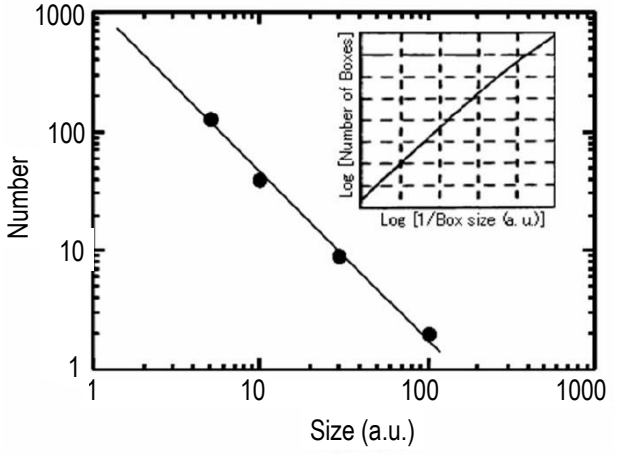

FIGURE 4: NUMBERS OF THE V-SHAPED STRUCTURES ARE PLOTTED AS A FUNCTION OF THE SIZE. THE INSET SHOWS THE RESULT OBTAINED THROUGH BOX COUNTING METHOD.

The self-similar, nested, hierarchical structures are to emerge from the pre-existing defects spreading throughout the active region when carriers are injected enough. Such hierarchical structure, being supported by energy inflow and dissipation, could be made not only in inorganic but also in organic or bio-related materials. Thus the self-organized criticality can be utilized as an approach beyond lithography for uniting bottom-up and top-down structures as discussed below.

III. CONNECTING BOTTOM-UP STRUCTURES WITH TOP-DOWN STRUCTURES

3.1 Primitive case

The present bottom-up system of the dislocations, being caused by spatio-temporal dissipation in LD structure, is a fully solid state system, in marked contrast to the sand system [14] or the diffusion-limited aggregation (DLA) system [15], and is accessible through an electronic manner. In Fig. 5, schematic view of the aforementioned dislocation region lying in the active layer of the degraded II-VI LD's is shown with possible scheme for making connection between the bottom-up structure and the top-down system of LD's. We can set the bottom-up structure of the fractal dislocation network to grow at arbitrary position in the top-down structure of LD's by controlling the position of the stacking fault (for example, by placing oxide spots or by putting high-melting-temperature metal patterning) at the designed places on the substrate. Then, in the grown layers, the pn-junction region with stacking faults has non-radiative recombination centers that serve to proliferate dislocation networks resulting in the self-organized hierarchical nested structure, the size of which, on the other hand, can be controlled by the amount of the electron-hole injection in the pn-junction region of the II-VI diodes.

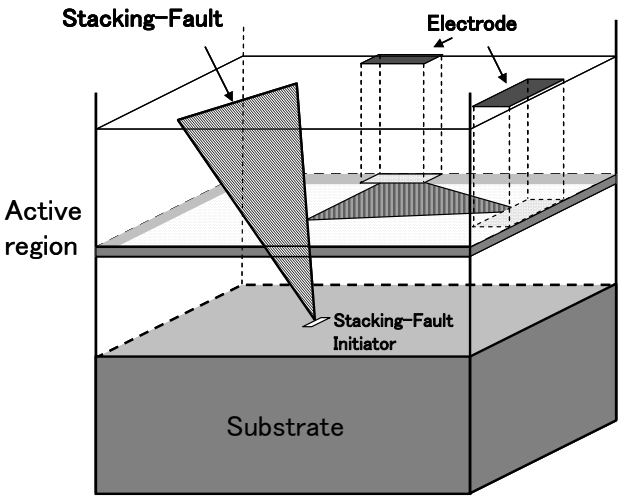

FIGURE 5 : SCHEMATIC VIEW OF THE TRIANGULAR DISLOCATION NETWORK SEEN IN A DEGRADED II-VI LASER DIODES.

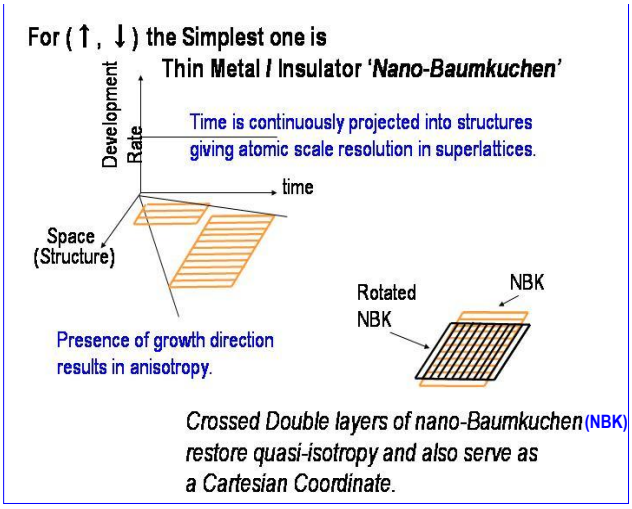

FIGURE 6: THIN ONE-DIMENSIONAL SUPERLATTICE AS A (↑,↓) STRUCTURE

3.2 More general case

In nanoscale, both a function derived from living matters and a function not derived from living matters can be reduced to a common interactive mechanism (ultimately to electromagnetic interactions). Therefore, a nanotechnology making remarkable progress contains latent importance of integrating non-living matters and living matters, but they have not yet been brought into full unification or union. Manufacturing methods of microstructures on the extension of conventional techniques include those using EUV or electron beam lithography and so-called bottom-up schemes using molecules, for example. However, there are no devices and systems that can couple them and try to find out synergy by the coupling. This is because, according to the above-introduced notation regarding the time-wise and space-wise characteristics, the bottom-up systems expressed by (time projectivity, spatial directionality)=(↑,↑) and the top-down systems denoted by (↓,↓) in the same notation have opposite natures, and it is difficult to find a good connection between them when just straightforwardly put side-by-side, i.e., (↑,↑) (↓,↓) for which, note that, there is a flip in the direction of the arrows. Thus it is just like oil and water, and incompatibility exists there. Coupling of the nanoscale world and the macroscopic world is the barrier that engineers must break through to couple new effects or functions that will be obtained in future in the field of nanotechnologies to existing silicon-based IT infrastructures and educing synergies. This problems can be solved by preparing a coupling intermediate layer or a coupling platform in which bottom-up and top-down systems are coupled. Specifically, the problems can be solved by inserting a system having the nature of (time projectivity, spatial directionality)=(↑,↓) as the third structure between a bottom-up system of (time projectivity, spatial directionality)=(↑,↑) and a top-down system of (time projectivity, spatial directionality)=(↓,↓). For this purpose, an accompanying line corresponding to a neuron system is provided in an artificial bottom-up system. Alternatively, a self-organized system is grown near an accompanying system prepared beforehand.

As shown in Fig. 6, growth of a one-dimensional superlattice [7] is brought about with time projected. Since the spatial coordinate in the growth direction of the one-dimensional super-lattice exhibits the flow of time directly, this can be regarded as a system in which time is projected continuously to the spatial structure along the growth direction. By using a controlled growth rate, or more preferably, a constant growth rate, the spatial structure is controlled continuously by time (coordinate). In addition, the spatial structure is anisotropic in that there are alternating hetero-layers along the growth direction while in the lateral direction there exists homogeneous layers of each slabs of the superlattice.

The one-dimensional superlattice grown in this manner is processed into thin pieces. The one-dimensional superlattice, having its thickness given by growth rate multiplied by the growth time, certainly has a structure in which the time t is woven into the growth direction. On the other hand, the superlattice, having alternating structure along the growth direction and homogeneous structure in lateral direction, is with an anisotropic structure. Thus, by processing the one-dimensional super-lattice into a thin piece, a system having the nature of (time projectivity, spatial directionality) = (↑,↓) can be realized (we denote the system as (↑,↓) for simplicity). As shown in right bottom in Fig. 6, the superlattice thin piece is superposed on

another similar superlattice thin film with a difference in orientation by an angle, for example, 90 degrees. By stacking two superlattice thin pieces, quasi (discrete) isotropy is recovered, and a Cartesian coordinate is formed simultaneously. Thereby obtained is a scheme permitting access to a space discretely as well as densely in nanoscale. With this, a mechanism that individually addresses an entirely continuous arbitrary (two-dimensional) bottom-up system can be made. That is, the thin superlattice structure (↑,↓) shares the time continuity with the bottom-up system (↑,↑) and shares the spatial anisotropy with the top-down system (↓, ↓). Therefore, the superlattice structure has good affinity to both the bottom-up system and the top-down system, and can unite those two otherwise hard-to-meet structures, through generating a system of (↑,↑) (↑,↓) (↓,↓), for which, note that, there is no flip in the direction of the arrows [16]. This scheme, being versatile, can be used to give a new category in *big data*. For example point of sales (POS) [17] data, being human-related as well as of consciousness, can be denoted as (↑,↑) , while IOT [18] data, being of things and therefore of no consciousness, are characterized by (↓,↓). Then the recently developed Kinetosomnogram (KSG) [19] exploiting the high cleanliness of clean unit system platform (CUSP) [20] has the property of (↑,↓), since KSG gives the data of human-beings when they are asleep. Thus, by generating the data base with the structure of (↑,↑) (↑,↓) (↓,↓), we can combine brain-related data with body-related ones in a highly sophisticated manner.

When we denote the man-made system [in which union of top-down and bottom-up, TD ∪ BU, is made] as (TD,BU), we can write

$$(TD,BU) \in \{TD\},\ (\text{ in general } (TD, (TD, (...(TD, BU)...)) \in \{TD\}), \quad (1)$$

where {TD} is a set of top-down systems, because the system (TD,BU) is one of the top-down system in that it is made under human designs. This is a sort of self-reference and is of potential interest when we think of the interaction of human's activities with Mother Nature.

3.3 Spiral heterostructure and its applications

For fabrication one-dimensional superlattice structure shown in Fig. 6, one way is to roll up a heterostructure. This technique can be used to fabricate new devices.

3.3.1 Quantum cross devices

First, the metal/insulator spiral heterostructure is fabricated using a vacuum evaporator including a film-rolled-up system. Then, two thin slices of the metal/insulator nano-baumkuchen are cut out from the metal/insulator spiral heterostructure. Finally, the two thin slices are attached together face to face so that each stripe crosses in a highly clean environment [20]. Utilizing this DNB structure, we can expect to realize high density memory devices, the crossing point of which can be scaled down to ultimate feature sizes of a few nanometers thanks to their atomic-scale resolution of the film thickness determined by the rate of metal deposition, ranging from 0.01 to 1 nm/s. One element of the double nano-"baumkuchen"(DNB) structure is called a quantum cross (QC) device, which consists of two thin metal films (nanoribbons) having the edge-to-edge configuration [21] as shown in Fig. 7 [22]. In this QC device, the area of the crossed section is determined by the film thickness, in other words 1-20 nm thick films can produce 1×1 nm^2-20×20 nm^2 nanoscale junctions. Since the vacuum evaporation has good spatial resolution of one atomic layer thickness, the size of QC could ultimately be as small as a few ångströms square (10^{-2} nm^2). Further, why scanning tunneling microscope (STM) can have atomic spatial resolution is because quasi-zero-dimensional (0D) space is generated between the sample's two dimensional surface and the STM head [23]. There is another way to make such "0D" space and that is by crossing two thin wires or edges of two thin ribbons. This situation is realized in the structure where two slices of the spiral hetero-structures are put together.

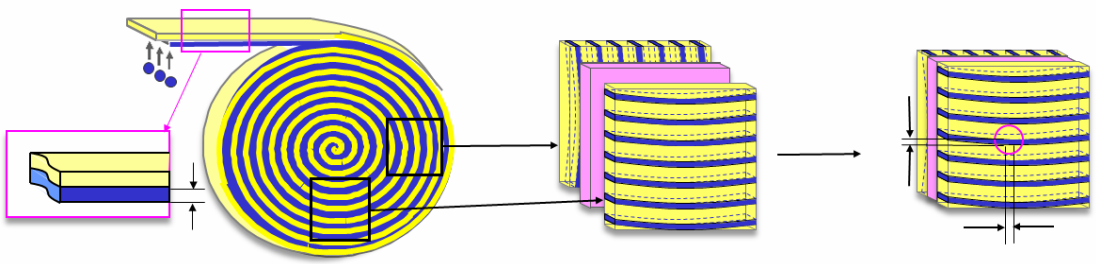

FIGURE 7: FABRICATION PROCEDURE OF DNB STRUCTURES

We have been investigating electrical properties of Ni/PEN films used as electrodes in QC devices and I-V characteristics for three types of QC devices as shown in Fig. 8 [22]. The three types of QC devices are as follows: (i) Ni/Ni QC devices (17 nm linewidth, 17×17 nm^2 junction area), in which two Ni thin films are directly contacted with their edges crossed, (ii) Ni/NiO/Ni QC devices (24 nm linewidth, 24×24 nm^2 junction area), in which NiO thin insulators are sandwiched between two Ni thin-film edges and (iii) Ni/P3HT:PCBM/Ni QC devices (16 nm linewidth, 16×16 nm^2 junction area), in which P3HT:PCBM organic molecules are sandwiched between two Ni thin-film edges. In our study, we have successfully fabricated various types of QC devices with nano-linewidth and nano-junctions, which have been obtained without the use of electron-beam or optical lithography. Our method will open up new opportunities for the creation of nanoscale patterns and can also be expected as novel technique beyond conventional lithography. Furthermore, we have presented the calculation results of the electronic transport in Ni/organic-molecule/Ni QC devices and discussed their possibility for switching devices. According to our calculation, a high switching ratio in excess of 100000:1 can be obtained under weak coupling condition. These results indicate that QC devices fabricated using thin-film edges can be expected to have potential application in next-generation switching devices with ultrahigh on-off ratios.

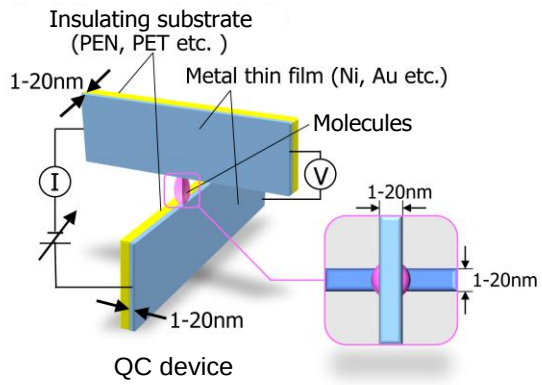

FIGURE 8: QUANTUM CROSS (QC) STRUCTURE CONSISTING OF TWO THIN METAL FILMS (NANORIBBONS) CROSSED WITH EDGE-TO-EDGE CONFIGURATION

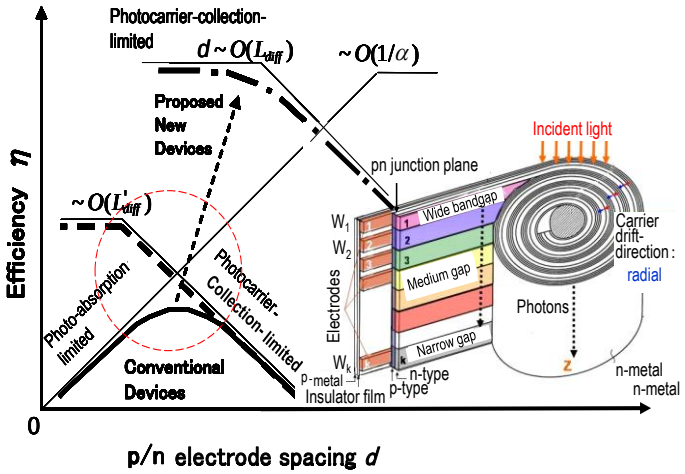

FIGURE 9: CONVERSION EFFICIENCY VS. ELECTRODE SPACING (SEIMICONDUCTOR THICKNESS). THE INSET DEPICTS THE MOP^{3}SL BASED ON SPIRAL STRUCTURE

3.3.2 Multi-striped orthogonal photon-photocarrier propagation solar-cell (MOP^{3}SL)

Based upon a spiral heterostructure, proposed is multi-striped orthogonal photon-photocarrier-propagation solar cells [24], in which the photons propagate in the direction orthogonal to that of the photocarrier's. One example of our new solar cells is, as shown in the inset of Fig. 10, based on the spiral heterostructure that is made by rolling up a pn junction sandwiched between anode electrode and cathode electrodes on a flexible substrate. In this solar cell, photons being absorbed in the direction vertical to the carrier drift/diffusion, the aforementioned trade-off can be lifted off to give the thick dash line in Fig. 10. In our solar cell, the direction of photon propagation is parallel to the axis of the disk (z-direction) and is orthogonal to photo-carriers' drift direction, i.e., the radial direction of the disk as shown in the inset. Thanks to the orthogonality, we can fully enjoy the freedom to make the disk thick enough to absorb all the photons keeping the distance between the p/n electrode distance (semiconductor layer thickness) thin enough to allow most of photocarriers to reach out to the contact metals. Moreover, we can utilize the degree of freedom along z direction. By, for example, printing multiple semiconductor stripes, we can prepare k semiconductor stripes, neighboring to each other, with different band gaps on the flexible substrate in such an order that the incoming solar photons first encounter the widest gap semiconductor, then narrower gap semiconductors, and the narrowest at bottom (inset of Fig. 9). With the optimized energy gaps (E_g=1.8eV, 1.3eV, 0.9eV, and 0.5eV) obtained in Fig. 10, we show, in the inset of Fig. 10, the limiting energy conversion efficiency as a function of the number of semiconductor stripes *k* for the multi-striped spiral-heterostructure solar-cell. We found that when the energy gap is carefully selected, we can obtain limiting energy conversion efficiency more than 50 % using four stripes of semiconductors.

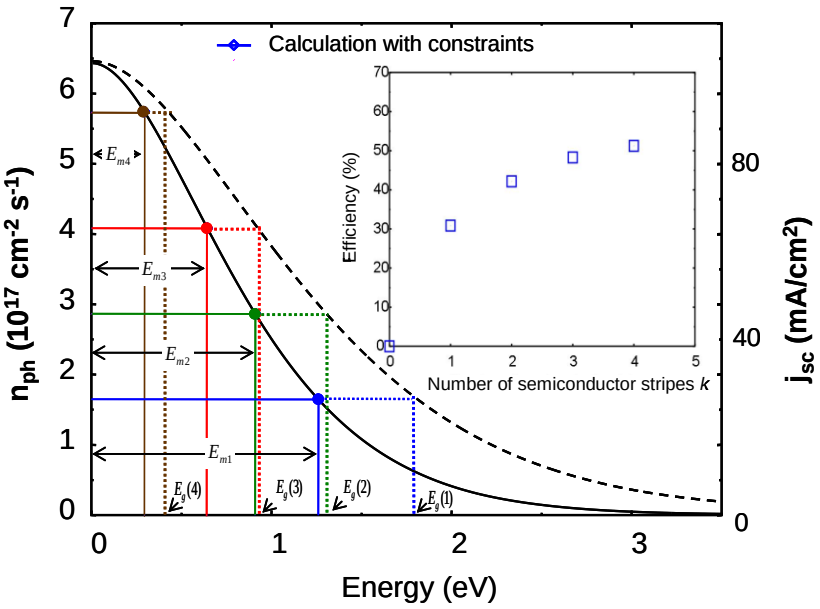

FIGURE 10: OPTIMUM ENERGY-GAP SELECTION FOR MULTI-STRIPED SPIRAL-HETEROSTRUCTURE SOLAR-CELL (FOR K=4)

Photons being impinging on the disk generating photo-carriers drifting in the radial direction, the photons propagate in a direction orthogonal to that of the photo-carrier's. Because of the orthogonality, the newly proposed solar cell can optimize the absorption of light and the photo-carrier collection independently and simultaneously without any tradeoff. The connected multi-striped spiral heterostructure-based solar cells can convert virtually the whole spectrum of black body radiation into the electricity with a single output voltage, being a candidate for the next generation solar cell with high energy conversion efficiency. The connected multi-striped spiral heterostructure-based solar cells can convert virtually the whole spectrum of black body radiation into the electricity with a single output voltage, being a candidate for the next generation solar cell with high energy conversion efficiency.

IV. UNITING TOP-DOWN WITH BOTTOM-UP ~ TOOL-BASED APPROACH

It will surely be necessary to perform cross-disciplinary experiments, especially uniting or unifying bottom-up systems with top-down systems through the fusion of cutting-edge research technologies such as semiconductor-based nano- technologies and bio- technologies in addition to flexible assembly processes. In this sense, the physics of having a clean environment becomes more important; many tools and processes commonly used in nanoscale research facilities, such as scanning probe microscopy (SPM), electrochemical material growth, photolithography, printing-technologies, chemical etching processes, molecular biology, and tissue culturing nowadays can basically be realized in a highly compact manner. Thus, in a tool/platform approach, for uniting bottom-up and top-down systems, we have developed clean unit system platform (CUSP).

Figure 11 shows how a conventional clean room [25, 26] works. Two sections are provided. One is a medium clean space where most routine processing is done. The other section is where a highly clean environment is realized, and, for example, photolithography of ultimate resolution is done. This section is, in a sense, a clean room in a clean room.

Obtaining high cleanliness and achieving high vacuum level have one aim in common, i.e. to draw the inner air off the chamber. To have a highly clean environment in a compact, inexpensive manner, we make a topological transformation starting from Fig. 11a. First we can merge the sidewalls in Fig. 11a and we have the one shown in Fig. 11b. Then, reducing the volume of the room and the size of the filtering system, we have the clean box shown in Fig. 11c. Obtaining high cleanliness and achieving high vacuum level also make a difference. For the vacuum system, it is a one-way process to pump the air out of the chamber, and the feed-back is not meaningful, but for the high cleanliness system it is. The system shown in Fig. 1c inhales air from outside through the inlet and exhales, through the outlet, the air cleaner than when inhaled. This is a waste of clean air. Thus, just like a turbo-engine in automobiles that exploits exhaust gas, we feedback the outlet air into the inlet together with making box airtight [20]. Now we have the system shown in figure 11e. Here we do a *gedanken-*

experiment with this system on how air is getting cleaned, and we note this system is equivalent to ultimate clean room system where infinite nesting is done as depicted in Fig. 11d.

Here, let us consider quantitatively how the conventional systems shown in Fig. 11a–c work. The particle (dust) density $n(t)$ in the chamber, i.e. clean room or clean box, changes under the left top equation given in Fig. 11, where V and S, σ, and N_o are, respectively, the volume, area of the inner surface of the chamber, rate of particles coming from the unit area per unit time, and the particle density of the environment where the conventional clean room itself is placed. Here, F is the volume of air put inside per unit time (i.e. flow) by a HEPA/ULPA fan filter unit, and γ is the filtration efficiency of dust particles by a single HEPA/ULPA filter. The power 2 in the third term in the differential equation is because the outdoor air passes through the filter twice in Fig. 11a, where for simplicity we assume a HEPA or ULPA filter has the same performance. The solution of the equation is given by the left middle equation with the boundary condition $n(0)= N_o$, i.e., the dust density in the clean room is initially in equilibrium with that of outside (ambient). As easily seen, we have the lowest dust density given by the left bottom equation in Fig. 11, as t goes to infinity. This is the same as the steady-state dust density, being obtained by putting $dn/dt=0$ in the left top equation in Fig. 11, tells us that n(t) is dependent on the ambient dust density N_o forever, and that high performance filter with γ close to one is indispensable in the conventional clean rooms.

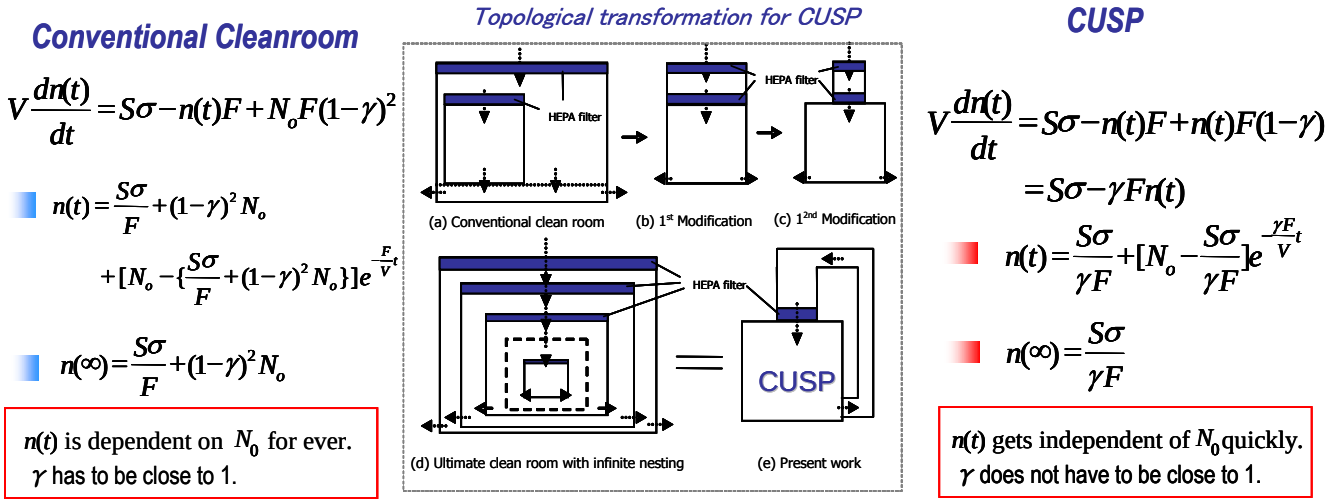

FIGURE 11: CONVENTIONAL CLEAN ROOM AND CUSP

In the case of Fig. 11e, however, we have the right top equation in Fig. 11, where the first and second terms in the middle sequence of the differential equation are identical to those in the left top equation, but the third term is different because the outgoing air is fed back into the chamber through the inlet. The solution, with the boundary condition $n(0)= N_o$, is given by the right middle equation. As time goes by, the second term quickly reduces down to zero, and the lowest (or, steady state) dust density n_s in our CUSP chamber shown in Fig. 11e is given by the right bottom equation, i.e.,

$$n_s = \frac{S\sigma}{\gamma F} \tag{2}$$

As seen in the right middle equation in Fig. 11, the dust density, thus, the cleanliness in CUSP chamber is indeed dependent on the ambient dust density at t =0, but soon at a time when $t/(V/\gamma F)$ ~ 20 or later, the second term in the right middle equation in Fig. 11 is negligibly small compared to the first term, i.e., the cleanliness in the CUSP chamber is then independent of the ambient dust density N_o, and is given by Eq. 2, which teaches us that in CUSP $n(t)$ becomes independent of the ambient dust density N_o quickly, and that small σ, not γ close to unity, is of importance.

The cleanliness that CUSP can realize is given in Fig. 12. The solid circles with error bars, in Fig. 12, show the cleanliness of the 2nd Generation CUSP (S-CUSP) [27]. It is found that the airborne particle concentration almost varies as d^{-2} with d the particle size, which is consistent with the analytical expression of the ISO standard. Based on the analyses of the experimental results, we have succeeded in obtaining the ultra-high cleanliness of ISO class -1 (minus 1) in the S-CUSP. This performance is four orders of magnitude better than that of a super clean room (ISO class 3).

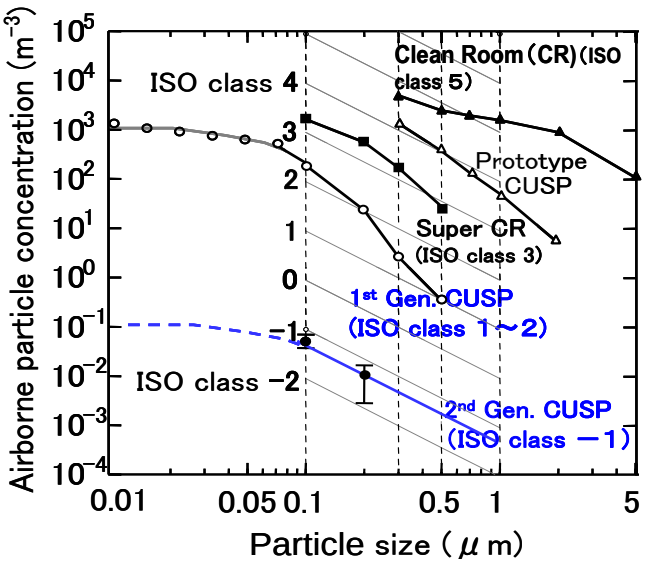

FIGURE 12: CLEANLINESS IN CLEAN ROOMS AND CUSPS

V. CONCLUSIONS AND PERSPECTIVES

As shown in Fig. 13, just like the string theory which enjoys explaining things seamlessly from large scale structures in universe to small entities with Planck scale by resolving the disaccord between the theory of relativity and the quantum theory, a possible platform that unites, or makes a bridge over the gap between, the top-down systems such as Si-based LSI's and bottom-up systems like self-organized or self-assembled systems will surely be able to enjoy as huge a success as the string theory does, because of its full seamless line-up of highly structured materials. First, we have to overcome the sharp contrast lying between the top-down system, whose structure is fabricated globally through man-made design from outside by so-called processing, and the bottom-up system, for which the structure, on the other hand, is determined autonomously through the local interactions described by non-equilibrium diffusion equations, etc. We have studied the possibility of creating a unification platform for bottom-up and top-down systems, which, as shown in Fig. 13, is one of the most important issues, in future, for harvesting fruits of upcoming nano-technologies and nano-science together with those of Si-LSI-based information technologies.

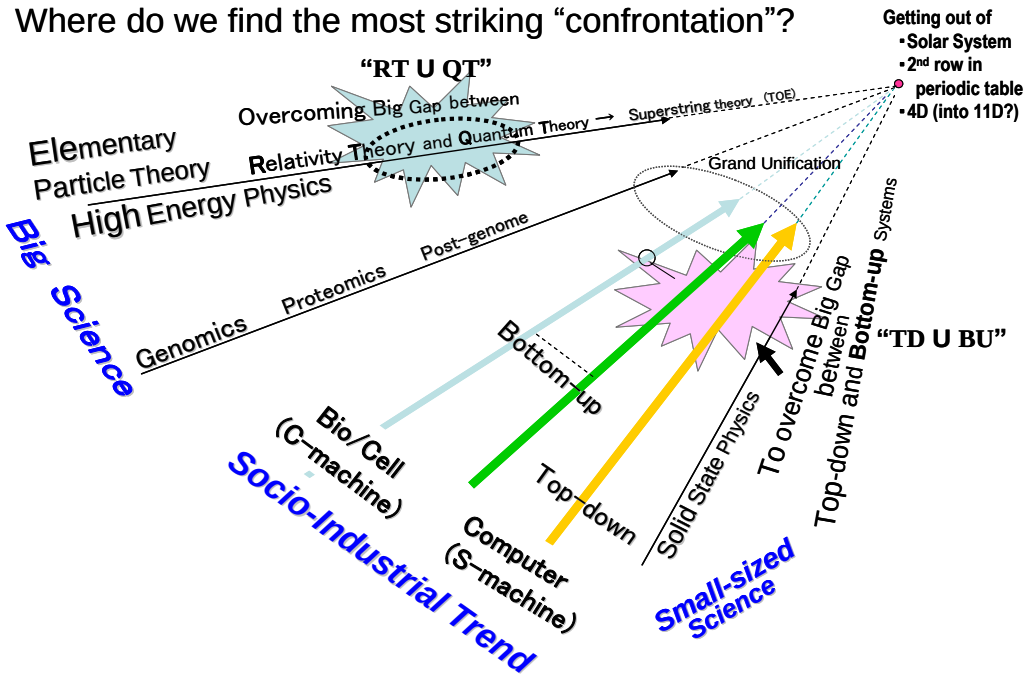

FIGURE 13: FUTURE PERSPECTIVES

Under the device based approach, for unifying bottom-up and top-down systems, proposed is a functional device that has hierarchical structures grown, or is to have hierarchical structures grow, inside, not as a result of top-down designing but as a result of self-organization, i.e., a bottom-up structure-formation. Such structure could be formed quite universally in many systems as long as they have inflow of energy as well as spatio-temporal dissipation. As already shown above, one of them is the pn-junction system, with which one can make an electronically controllable, self-similar, fractal (nested) structure, in a fully solid state system exploiting self-organized criticality induced by carrier injection and non-radiative recombination. What is demonstrate here, we believe, is to make otherwise inaccessible self-organized structures accessible, for the first time, in a fully solid state system, through electronic means that have huge affinity to established semiconductor electronics. The self-similar, nested, hierarchical structures are to emerge from the pre-existing defects spreading throughout the active region when carriers are injected enough. Such hierarchical structure, being supported by energy inflow and dissipation there, could be made not only in inorganic but also in organic or bio-related materials. As described above, according to the presented framework, it would be possible in near future to realize a sophisticated functional device that can make the best use of advantages of bottom-up systems and top-down systems represented by silicon LSI. Under the tool-based approach, for unifying bottom-up and top-down systems, clean unit system platform (CUSP) is developed. The clean versatile environments having small footprint, low power-consumption and high cost-performance can be realized with CUSP for the next generation production system as well as for cross-disciplinary experiments. Multiply-connected CUSP system based upon those would serve as the platform not only for nano-technologies or bio-technologies but also for the next-generation environment-friendly platform for industries. In terms of small footprint, low power-consumption and high cost-performance, CUSP in its full line-up could outperform a conventional super cleanroom ("main frame") and would be the *cleanroom for all of us*.

The author express sincere thanks to Drs. Y. Mori, S. Tomiya, S. Ito, K. Nakano, H. Okuyama, K. Kondo, and H. Kaiju for fruitful discussions, This work is supported, in part, by Special Education & Research Expenses from Post-Silicon Materials and Devices Research Alliance, JST Seeds Innovation Program, Post-Silicon Materials and Devices Research Alliance, Nano-Macro Materials, Devices and System Research Alliance, and 2010-2012 Grant-in-Aid for Scientific Research (B) [22350077], 2013-2015 Grant-in-Aid for Scientific Research (B) [25288112], 2016-2018 Grant-in-Aid for Scientific Research (B) [16H04221], and 2016-2017 Grant-in-Aid for Challenging Research (Exploratory) [16K12698] from the Japan Society for the Promotion of Science (JSPS).

REFERENCES

[1] W. H Brattain and J. Bardeen, "Three-Electrode Circuit Element Utilizing Semiconductive Materials". U.S. Patent 2,524,035 (1947)

[2] R. Noyce, "Transistor structure and method" U.S. Patent 2,929,753 (1960)

[3] J. Kilby, "Miniature Semiconductor Integrated Circuit", U.S. Patent 3,115,581 (1959)

[4] R. R. Llinas, "The Biology of the Brain", W.H. Freeman & Company, NY, p. 94 (1989)

[5] S. Wolfram, A New Kind of Science, Wolfram Media Inc., IL, USA (2002)

[6] P. Nemethy, P. Oddone, N. Toge, and A. Ishibashi, "Gated time projection chamber", *Nuclear Instruments and Methods* **212** 273-280 (1983)

[7] A. Ishibashi, "MOCVD-grown Atomic Layer Superlattices", *Spectroscopy of Semiconduc-tor Microstructures, eds.* G. Fasol, A. Fasolino, P. Lugli, Plenum Press, NY. (1989)

[8] Y. Chen, D. A. A. Ohlberg, X. Li, D. R. Stewart, R. S. Williams, J. O. Jeppesen, K. A. Nielsen, J. F. Stoddart, D. I. Olynick, and E. Anderson, "Nanoscale molecular-switch devices fabricated by imprint lithography", Appl. Phys. Lett. **82** 1610-1612 (2003)

[9] A. Ishibashi, Japanese Patent Laid-open Publication No. JP2000-2 1 6499, Pamphlet of International Publication No. WO 02/35616 (2000)

[10] T. Yoro, "Yuinoron", Seidosha, Tokyo (1989)

[11] P. Petroff, "Defects in III–V Compound Semiconductors", *Semiconductors and Insulators*, **5** 307 (1983)

[12] S. Guha, J. M. DePuydt, M. A. Haase, J. Qiu, and H. Cheng, "Degradation of II-VI based blue- green light emitters", *Appl. Phys. Lett.*, **63** 3107-3109 (1993)

[13] S. Tomiya, E. Morita, M. Ukita, H. Okuyama, S. Itoh, K. Nakano, and A. Ishibashi, "Structural study of degraded ZnMgSSe blue light emitters", *Appl. Phys. Lett*., **66** 1208-1210 (1994)

[14] P. Bak, C. Tang, and K. Wiesenfeld, "Self-organized criticality: An explanation of the 1/f noise", *Phys. Rev. Lett*. **59** 381-384 (1987)

[15] W. Wen and K. Lu, *Phys. Rev. E,* "Electric-field-induced diffusion-limited aggregation", **55** R2100-2103 (1997)

[16] A. Ishibashi, "Functional device, manufacturing method thereof, functional system, and functional material", US 2006/0088029 (2006)

[17] M. Kitazawa, T. Yamada, M. Takahashi, G. Yamamoto, A. Yoshikawa, T. Terano, and T. Fujino, "Analyzing In-store Shopping

Paths from Indirect Observation with RFID Tags Communication Data", *RISUS – Journal on Innovation and Sustainability*, **5**, 88-96 (2014)

[18] www.internetsociety.org, https://www.internetsociety.org/sites/default/files/ISOC-IoT-Overview-20151014_0.pdf

[19] A. Ishibashi and M. Yasutake, "Clean Unit System Platform (CUSP) for Medical/Hygienic Applications", *Int. J. Eng. Sci*., **2** 92-97 (2016)

[20] A. Ishibashi, H. Kaiju, Y. Yamagata, and N. Kawaguchi, "Connected box-units-based compact highly clean environment for cross-disciplinary experiments platform", *Electron. Lett.* **41** 735-736 (2005)

[21] A. Ishibashi, *Proceedings of International Symposium on Nano Science and Technology*, pp. 44-45, Tainan, Taiwan (2004)

[22] H. Kaiju, A. Ono, N. Kawaguchi, and A. Ishibashi", Ultrasmooth Ni thin films evaporated on polyethylene naphthalate films for spin quantum cross devices", *J. Appl. Phys.* **103** 07B523 (2008)

[23] A. Ishibashi and K. Kaiju, "Sonde, Methode zur Herstellung einer Sonde, Sonden-Microskop, Magnetkopf, Methode zue Herstellung eines Magnetkopf und einer magnetischen Aufnahme- und Wiedwergabevorrichtung", P41892/DE (2011)

[24] A. Ishibashi, N. Kawaguchi, K. Kondo, H. Kaiju, and S. White, "Spiral-heterostructure-based new high-efficiency solar cells", *Proc. Int. Symp. Environment. Consci. Design and Inv. Manufact*. (*EcoDesign2009)*, pp. 55-58 (2009)

[25] W. White, Cleanroom design, Wiley, Chichester, UK. (1999)

[26] T. Ohmi, "ULSI reliability through ultraclean processing", *Proc. IEEE*, **81** 716-729 (1993)

[27] Md. D. Rahaman, H. Kaiju, N. Kawaguchi, and A. Ishibashi, "Ultra-High Cleanliness of ISO Class Minus 1 Measured in Triply Connected Clean-Unit System Platform", *Jpn J. Appl. Phys*. **475** 5712-5716 (2008).